BOLETIN DE LA SOCIEDAD ESPAÑOLA DE
Cerámica y Vidrio
ARTICULO DE REVISIÓN

Mechanical behaviour of structural ceramics

S. BUENO, C. BAUDÍN

Instituto de Cerámica y Vidrio (CSIC). C. Kelsen 5,
28049 Madrid (España)

The use of ceramic materials in structural applications is limited by the lack of reliability associated with brittle fracture behaviour. In order to extend the structural use of ceramics, the design of microstructures which exhibit flaw tolerance due to toughening mechanisms which produce an increase in crack growth resistance during crack propagation has been proposed.
This work is a review of the mechanical behaviour of structural ceramic materials and its characterisation. Firstly, the basic brittle fracture parameters and the statistical criteria to determine the probability of exceeding the safety factors demanded for a particular application are analysed. Then, the toughening mechanisms which can be developed in the materials through microstructural design as well as the mechanical characterisation of toughened ceramics are discussed. The experimental values of linear elastic fracture toughness parameters (critical stress intensity factor, K_{IC}, and critical energy release rate, G_{IC}) are not intrinsic properties for toughened materials and depend on crack length and the loading system. In this work, the different mechanical parameters proposed to characterise such materials are reviewed. The following fracture parameters are analysed: work of fracture (γ_{WOF}), critical J-integral value (J_{IC}) and R-curve. For the determination, stable fracture tests are proposed in order to ensure that the energy provided during the test is no more than the necessary one for crack propagation.

Keywords: Microstructure, Strength, Weibull modulus, Fracture toughness, Toughening mechanisms.

Comportamiento mecánico de materiales cerámicos estructurales

El uso de los materiales cerámicos en aplicaciones estructurales está limitado por la falta de fiabilidad asociada a su comportamiento frágil durante la fractura. Para extender su aplicación se ha propuesto el diseño de microestructuras que presenten tolerancia a los defectos debido a la actuación de mecanismos de refuerzo.
Este trabajo es una puesta al día sobre el estudio del comportamiento mecánico de los materiales cerámicos estructurales y su caracterización. En primer lugar, se revisan los parámetros de fractura utilizados para caracterizar materiales frágiles y los criterios de control estadístico que permiten determinar la probabilidad de que se sobrepasen los factores de seguridad exigidos en cada aplicación. A continuación, se discuten los mecanismos de refuerzo que se pueden desarrollar en los materiales cerámicos a través del diseño microestructural.
En los materiales cerámicos en los que la actuación de mecanismos de refuerzo conduce a un comportamiento significativamente distinto del puramente frágil, los parámetros derivados del tratamiento lineal elástico (factor crítico de intensidad de tensiones, K_{IC}, y tasa crítica de liberación de energía, G_{IC}), determinados experimentalmente, dejan de ser propiedades intrínsecas del material, independientes del tamaño de grieta y el sistema de carga. El presente trabajo revisa los parámetros mecánicos propuestos para la evaluación de la tenacidad de fractura de los materiales cerámicos reforzados y los métodos utilizados para su determinación. Se analizan los siguientes parámetros mecánicos: trabajo de fractura (γ_{WOF}), valor crítico de la integral J (J_{IC}) y curva R. Para su determinación se proponen ensayos de fractura estable, que aseguran que la energía suministrada durante el ensayo se emplea únicamente en la propagación de la grieta.

Palabras clave: Microestructura, Tensión de fractura, Módulo de Weibull, Tenacidad de fractura, Mecanismos de refuerzo.

1. INTRODUCTION

A large number of non-metallic inorganic materials obtained through substantial refining or modification of the initial raw materials with a view to obtaining specific properties for each application are classified under the name of advanced ceramics (1). This name includes functional materials with electric, electronic and magnetic applications, amongst others, and structural materials whose main function is to stand mechanical stresses at room or at high temperatures.

Ceramic materials have a series of advantages in comparison with metallic and plastic materials for structural applications, such as their resistance to corrosion and wear and the fact that they maintain high resistance to deformation at temperatures at which other materials develop generalized flow phenomena. The mechanical behaviour of ceramic materials is an important field of study for both the development of structural ceramic components and for functional ceramics, since the mechanical stresses acting on a particular functional component can be sufficient to produce its failure.

The type of fracture of a material subjected to stress is determined by its capacity to deform plastically, which depends on temperature. Generally speaking, metals present ductility at room temperature, while the majority of ceramic materials are characterized by the absence of plastic deformation up to relatively high temperatures, due to the highly directional covalent-ionic bond. For example, alumina (Al_2O_3) presents no evidence of dislocation movement up to temperatures of over 900ºC and silicon nitride (Si_3N_4) reaches sublimation temperature without experiencing plastic phenomena (2). Thus, the form of fracture of ceramic materials is fundamentally brittle, with Mode I or opening mode, the most common fracture mode (Fig.1).

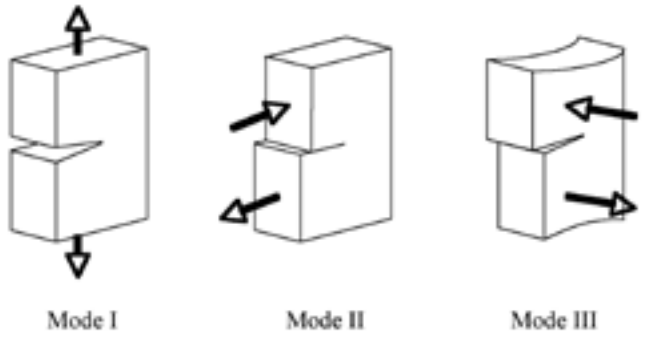

Fig. 1- Fracture modes. Ceramics usually fail in mode I.

Brittle behaviour is characterized because the stress level at which the start of fracture occurs is determined by the presence of defects which act as stress concentrators, producing the catastrophic failure in the material. Thus, the strength of brittle materials is a highly variable property, which depends on the presence and on the distribution of flaws. Moreover, the strength values are much lower than the theoretical fracture stress, or stress necessary to separate two atomic planes of the material. The theoretical fracture stress, evaluated on the basis of the simplified model of two atoms is of the order of $10^{-1}\cdot E$, where E is the material's Young´s modulus (3) and, in general, the strength values of ceramic materials are around $10^{-2}\cdot E$ and $10^{-3}\cdot E$ for single-crystal fibres and dense fine-grain polycrystalline materials respectively.

To minimize brittle behaviour, it is essential to understand how the material's microstructure determines its mechanical behaviour and how the microstructure can be engineered to enhance mechanical response. Attempts have traditionally been made to improve this behaviour by using processing techniques where the size and the quantity of flaws leading to the failure of the material are reduced. This approach has a limitation, since the complete elimination of flaws is in practice impossible, particularly during mass production. Thus, the designing of microstructures and/or structures which can sustain toughening mechanisms and make materials more flaw-tolerant is sought (4-7).

The study of the mechanical behaviour of materials is a wide discipline which analyzes their response under mechanical stresses. When the materials are in use, these stresses may imply not only static or variable loads, eventually combined with corrosion processes (8, 9) but also temperature-related dilatational stresses (10,11). Frictional stresses, which occur during the interaction of solid surfaces in movement, are the object of tribology. The wear or damage which occurs on the surfaces, generally in the form of material loss, is critical for overall material behaviour (12-13).

This work is a review of the mechanical behaviour of structural ceramic materials and its characterization. It will only consider the basic properties which describe the fracture of materials and determine their response under normal working conditions. Firstly, the fracture parameters used to characterize brittle materials are analyzed. The statistical control criteria that make it possible to determine the probabilities of failure of pieces subjected to different stress levels are considered. Then, the toughening mechanisms which can be developed in ceramic materials through microstructural design together with the fracture parameters which make it possible to characterize toughened materials are reviewed.

2. BASIC MECHANICAL PARAMETERS FOR BRITTLE MATERIALS

Since the stress values at which break a series of pieces of a brittle material which are nominally the same and are subject to identical stresses, are extremely variable, it is impossible to use the average value of strength as an intrinsic parameter which characterizes the fracture of the material. Linear Elastic Fracture Mechanics (LEFM, review in refs. 14-16), largely developed in the first half of the 20th century, analyzes the fracture of brittle materials with a view to separating the contribution of the flaws present from that of their intrinsic properties, determined by the microstructure, to the strength values. This separation gave rise to the concept of fracture toughness as the material's resistance to the propagation of defects, determined by its microstructure and independent of the particular flaws present in it.

2.1. Fracture toughness

There are two basic approaches to the concept of fracture toughness: the approach based on an energy criterion and the approach based on the evaluation of the distribution of stresses around a flaw, or criterion based on the stress intensity factor.

According to Griffith's energy principle (17), the flaws present in a body subjected to load are propagated to reduce the system's energy through the formation of two new fracture surfaces. Thus, the propagation of a crack is governed by the relationship between the elastic deformation energy stored in the system which contains the crack, and the surface energy required to form new surfaces, G, which, in totally brittle materials, would be equal to twice their thermodynamic surface energy (γ_0) On the basis of this principle, the fracture stress, σ_f, of a body which breaks because of the propagation of a crack of size c, is determined by (Eq. 1):

$$\sigma_f = Z\cdot\left(\frac{2\cdot E'\cdot\gamma_0}{c}\right)^{1/2} \qquad [1]$$

where E′ is the generalized elastic modulus of the material, equal to E for plane stress and $E'=E/(1-\upsilon^2)$ for plane strain (E is the Young´s modulus and υ is the Poisson's ratio) and Z is an adimensional constant which depends on the geometry of the flaw and the load system.

In the energy balance proposed by Griffith, the G parameter

is defined as specific energy available for the fracture or energy release rate. The value of G at the time fracture starts is known as the critical energy release rate, G_{IC} in mode I, which is equal to the energy released by unit of extension of the crack front and by unit of body thickness, equal to $2\gamma_0$ for brittle materials (Eq. 2):

$$G_{IC} = 2\gamma_0 \quad [2]$$

Thus, G_{IC} is an intrinsic property which characterizes resistance to crack propagation or the material's fracture toughness.

As Davidge (3) indicates, the surface energy of fracture in real materials is higher than the thermodynamic surface energy, due to deviations from ideal perfectly brittle behaviour. Consequently, the fracture of the material is determined by effective surface energy at the start of fracture (γ_I, in mode I) which is the sum of the contribution of several terms. In addition to γ_0, the following contribute in a polycrystalline material: the effect of the not flat fracture surfaces, inelastic deformation of the areas adjoining the fracture surfaces, possible subsidiary cracking connected to the main crack and other phenomena, such as heat or sound, which are difficult to quantify. The value of γ_I is conditioned by grain size and fracture mode, since the energy consumed during the transgranular fracture is different from the energy of fracture through the grain boundary (3,18). Because of the diversity of contributions affecting γ_I it is impossible to quantify theoretically its value in polycrystalline materials and so must be determined experimentally.

Subsequent to Griffith's theory, the approach based on the stress intensity factor was developed. According to this approach, in a material subjected to a stress, σ_A, the stresses and deformations on the crack front are related by a universal proportionality factor called stress intensity factor. For ceramic materials which break in Mode I, we have (Eq. 3):

$$K_I = Y \cdot \sigma_A \cdot \sqrt{c} \quad [3]$$

where K_I is the stress intensity factor in Mode I, c is the crack length and Y is an adimensional factor depending on the geometry of the loading system and the crack. The crack is propagated when the stress intensity factor reaches a critical value, K_{IC}, which depends exclusively on the material. Thus, this critical value is a measure of the material's fracture toughness.

A dimensional analysis, initially conducted by Irwin (19), considered that fracture starts when the stress, σ_A, and the stress intensity factor, K_I, reach their critical values, σ_f and K_{IC}. This made it possible to establish a relationship of similarity between fracture toughness deriving from the energy criterion and the criterion based on the stress intensity factor and, thus, the equivalence of the two criteria (Eq. 4).

$$G_{IC} = \frac{K_{IC}^2}{E'} = 2\gamma_I \quad [4]$$

It can be derived from this equivalence that the fracture toughness of brittle materials is characterized by any of the three parameters, K_{IC}, G_{IC} or γ_I. These three parameters are defined at the start of propagation of the crack and are intrinsic properties of the materials, which do not depend on the load system or on the geometry of the cracks.

2.2. Critical flaw

A critical flaw is the name given to a defect which causes the fracture of a piece of brittle material (size c in Eqs. 1 and 3) when it is propagated. In glasses where there are no microstructural characteristics which modify the propagation of the cracks, the flaw causing the fracture is surrounded by four clearly distinguishable regions (Fig. 2). Surrounding the defect is the mirror region, with a totally smooth fracture, formed when a single crack is propagated on a plane perpendicular to the applied stress. When the crack is propagated and forms the mirror region, it accelerates until it reaches a critical speed at which different points on the front of the crack begin to propagate themselves on different planes, increasing the roughness of the fracture and producing the mist region. This tendency towards propagation on different planes increases until significant ramification of the main crack occurs; the roughness of the fracture surface increases progressively from the hackle region to the crack branching region where striations can be clearly seen. The degree of ramification of the main crack depends on both the speed of its propagation and on the energy release rate during fracture,

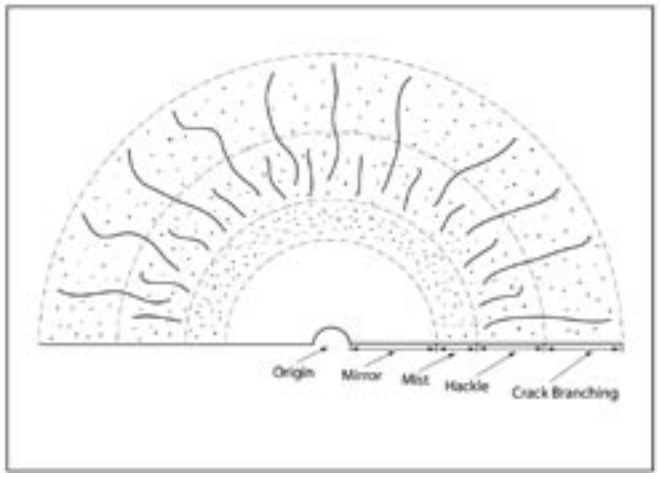

Fig. 2- Schematics of the fracture surface in glasses. The critical flaw is surrounded by the four well differentiated regions of different bumpiness signalled. Crack deviation and branching increase with distance to the critical flaw, up to the crack branching region where extensive striation is observed.

and is higher in fractures corresponding to high fracture stress values and small size cracks, which are accompanied by greater energy (20).

In polycrystalline materials, the micromorphology of the crack is influenced by the microstructure, which implies that the areas represented in Fig. 2 are not always identified (Fig. 3). Generally speaking, this identification is much easier the smaller the grain size and the greater the proportion of transgranular fracture. Figures 4 and 5 show fracture surfaces characteristic of structural ceramic materials where three regions are observed. These surfaces are similar to those observed in glasses, with more or less tortuous fracture, depending on the distance from the flaw. In these cases, the mirror region always presents some roughness, determined by the micromorphology of the fracture.

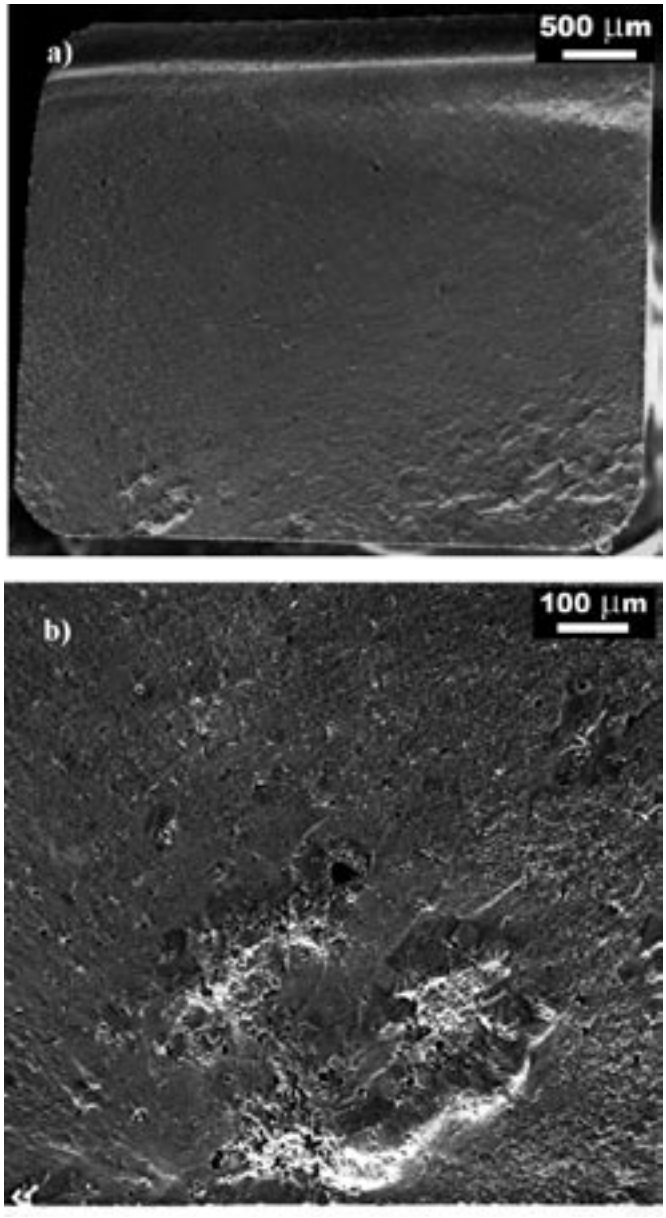

Fig. 3- Characteristic fracture surface of structural ceramics with low strength values. Bar (3x4x50 mm^3) of a spinel of aluminium and magnesium material tested in 4 points bending (40-20 mm). The zone of the specimen in tension during testing is located at the bottom of the micrographs obtained by scanning electron microscopy. a) General view. The regimes shown in Fig. 2 are not clearly observed, as it is characteristic of low energy fractures associated with low strength materials. b) Detail of the critical flaw developed by differential sintering: a group of pores associated to high density areas.

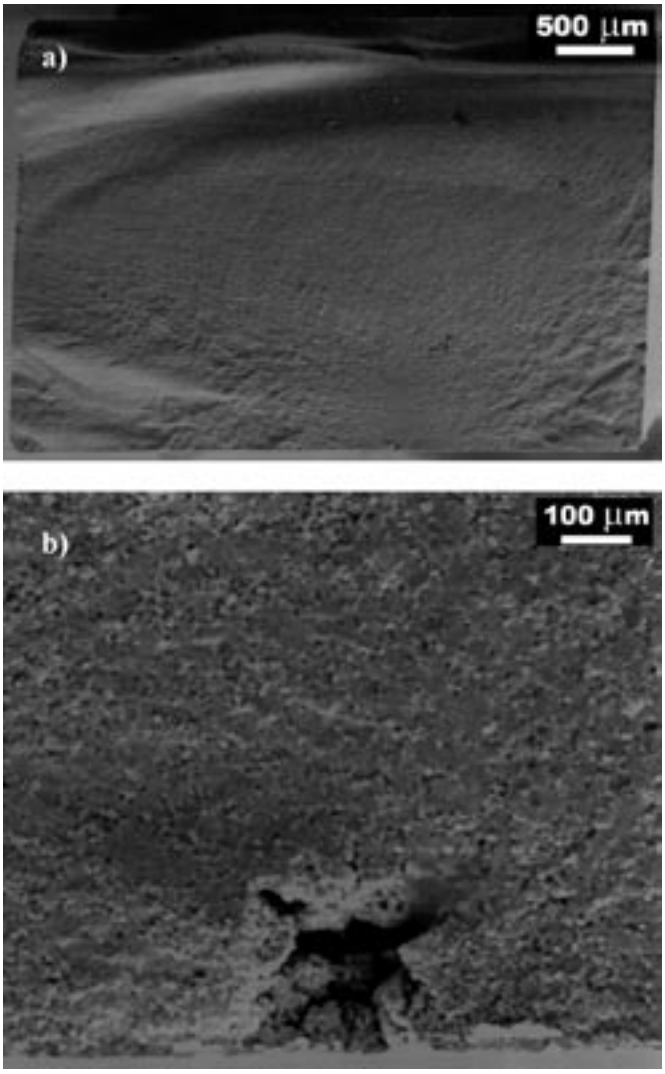

Fig. 4- Characteristic fracture surface of structural ceramics with high strength values. Bar (3x4x50 mm^3) of an alumina material tested in 4 points bending (40-20 mm). The zone of the specimen in tension during testing is located at the bottom of the micrographs obtained by scanning electron microscopy. a) General view. The regimes shown in Fig. 2 are observed. b) Detail of the critical flaw: a pore formed by differential sintering of agglomerates.

Flaws can be classified in two large groups: extrinsic and intrinsic (20). Extrinsic flaws originate during the machining of the parts, from impact, wear or corrosion during use, etc. Intrinsic flaws are the defects present in the microstructure of the material. In an ideal totally dense polycrystalline material, the actual grains of the material would constitute the critical flaws, since the grain boundaries are low-density regions, where defects are concentrated during sintering of the materials. However, when the fracture surfaces of ceramic materials are analyzed, flaws that are larger than the grain defect are generally encountered, like those shown in Figure 3-5, which are produced during sintering generally due to microstructural defects present in green compacts. In this sense, it is very important to underline the so-called "memory effect" of ceramic materials. Since the formation of liquids in ceramic compound mixtures takes place at high temperatures, the manufacture of ceramic components is largely done through powder technology at room temperature and subsequent thermal treatment. In the latter stage, the materials are sintered. This occurs because of the transport of mass in solid state in the majority of cases and, consequently, the homogenization related to metal or glass fusion processes does not occur. In addition to differences in composition, deriving from a deficient mixture of the raw materials or from contamination from undesired species, the intrinsic flaws observed in ceramic materials are pores (Figs. 4 and 5) or groups of pores (Fig. 3), cracks and regions of high density, normally associated with pores and cracks (Fig. 3-4). The

high-density regions are formed during the thermal treatment because of the differential sintering of agglomerates present in the green compacts and tend to be associated with pores.

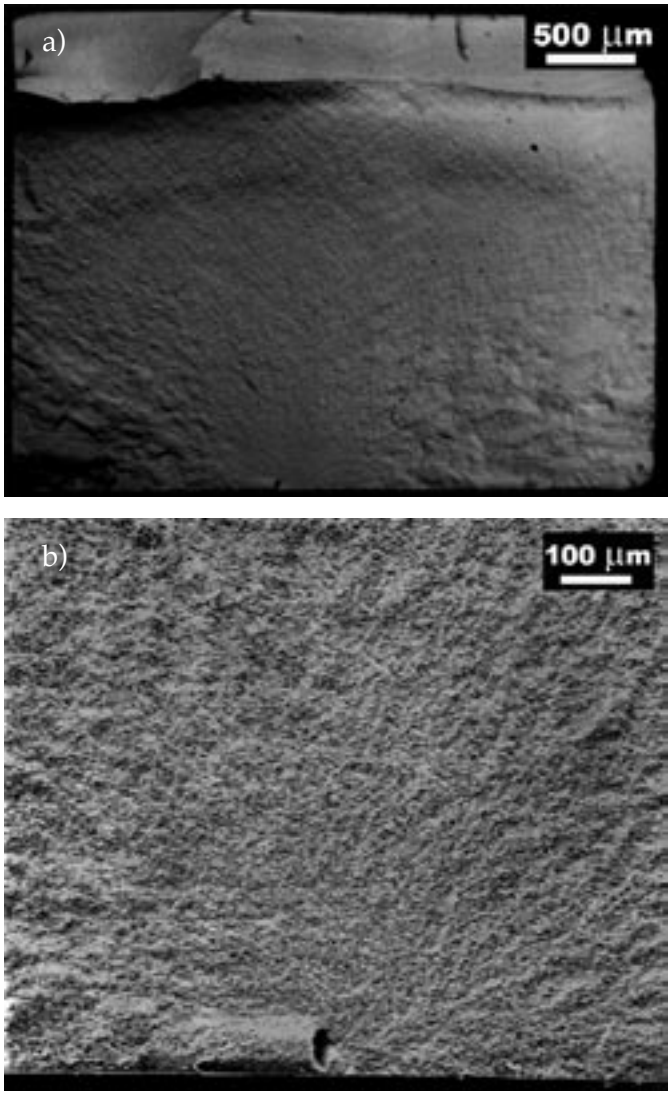

Fig. 5- Characteristic fracture surface of structural ceramics with high strength values. Bar (3x4x50 mm^3) of an alumina+10vol.% of aluminium titanate material tested in 4 points bending (40-20 mm). The zone of the specimen in tension during testing is located at the bottom of the micrographs obtained by scanning electron microscopy.
a) General view. The regimes shown in Fig. 2 are observed.
b) Detail of the critical flaw: a pore developed during sintering from porosity present in the green state.

Moreover, pores can be formed due to the evolution of the porosity of the green compact (Fig. 5).

In addition to the microstructural defects mentioned above, the residual stresses developed during cooling from the sintering temperature may be very substantial in ceramic materials. These stresses originate on the boundary between grains of phases with different coefficients of thermal expansion (CTE) or between grains of a single phase which presents anisotropy in the CTE. In addition, the phase transformations with associated volumetric changes produce residual stresses which can lead to microcracking of the material during cooling and, thus, to a reduction in strength values. Moreover, they can act jointly with the applied stress and modify the behaviour of grain boundaries. Control of residual stresses can be the origin of toughening mechanisms during the fracture of the materials, as is discussed in section 3.2.

2.3. Distribution of strength values

Since fracture of ceramic materials originates from flaws which act as stress concentrators, the stress values at which a set of nominally identical pieces under the same load conditions break show wide dispersion, which in many cases could be as much as 100%. This does not happen with ductile materials; for example, the dispersion observed in metals is of 4-8%. Thus, the average value of strength can be used as a design parameter in ductile materials but not in brittle materials, where a detailed analysis of the breakdown of the values of this parameter is necessary to determine the probability of the safety factors required in each application being surpassed.

Critical flaws in ceramic materials have different shapes and sizes and are located and oriented in the piece in different ways with respect to the applied stress. These characteristics alone would already produce highly variable values for the strength but also, as can be observed in Figures 3-5, the flaws can be of a very different nature. It is then not possible to forecast the behaviour of a ceramic component in fracture on the basis of the analysis of its microstructure. Consequently, the population characteristics of the fracture stress values must be determined through experiments.

TABLE I. STRENGTH OF SOME STRUCTURAL CERAMICS AS A FUNCTION OF TESTING METHOD AND SPECIMEN SIZE. (21-23). B=WIDTH, H=HEIGHT

Sintered Si_3N_4 (21)					
Method	Span (mm)	Specimen dimensions (mm)	σ_m (MPa)	$\Delta\sigma_{max}$ (MPa)	σ_{min} (MPa)
3 points bending	L=10	b=4 h=2	638	718	493
	L=30	b=4 h=3	492	598	358
4points bending	L_1, L_2=30, 10	b=4 h=3	391	478	324
		b=8 h=4	357	430	297
Hot pressed Si_3N_4 (22)					
Method	σ_m (MPa)				
3 points bending	861				
4points bending	689				
Uniaxial tension	413				
Hot pressed Si_3N_4 (23)					
Method	Span (mm)	Specimen dimensions (mm)	σ_m (MPa)		
3 points bending	L=38	b=6,4 h=3,2	930		
4points bending	L_1, L_2=38, 19		724		
Uniaxial tension			552		

As can be derived from the results shown in Table I (21-23), the average strength values of ceramic materials fall as the size of the specimens increases and show a great dependence on the mode of loading. The average value decrease as the number of pieces tested increases. This type of behaviour is very different from what has been found in the majority of materials properties: their experimental values generally follow Gaussian-type distributions, where an increase in the number of determinations produces a decrease in dispersion with no change in the average value.

As has already been discussed, brittle materials break catastrophically, without the load being redistributed, due to the propagation of the flaw which produces the greatest stress intensity in the piece due to the effect of the applied stress. Weibull (24) analyzed this type of behaviour on the basis of the principle of the weakest link: a chain formed by n links breaks if any of the n links breaks. As Weibull points out, this principle is applicable to a wide number of problems where whatever causes an event in any part of the whole implies that it will occur in the whole.

Using the general form of the Weibull function, the probability of failure, $P_f(\sigma)$, of a volume V of material subjected to a uniaxial tension, σ, is given by (Eq. 5):

$$P_f(\sigma) = 1 - \exp\left(-V \cdot \left(\frac{\sigma - \sigma_u}{\sigma_{0V}} \right)^m \right) \quad [5]$$

where m is the Weibull modulus, σ_u, is the value of the stress for which the probability of failure is zero and σ_{0V} is a normalizing constant. Weibull points out that the value of this distribution resides in the fact that it is the simplest way of describing the observed behaviour, with the parameters m, σ_u and σ_{0V} having no physical content. Later analyses by Jayatilaka and Trustrum (25) related the values of m with the width of the size distribution of the flaws present in the material.

For pieces subjected to non-uniform stress distributions, such as prismatic bars tested in bending which are used to determine fracture stress values, Equation [5] takes the form (Eq. 6):

$$P_f(\sigma) = 1 - \exp\left(-\int \left(\frac{\sigma - \sigma_u}{\sigma_{0V}} \right)^m dV \right) \quad [6]$$

On the basis of the Weibull analysis, the effect of the size of the pieces and mode of loading arises naturally. The average fracture stress value, σ_{fm}, is given by Eq. [7] (25):

$$\sigma_{fm} = \frac{\sigma_{0V}}{V^{1/m}} \cdot \Gamma\left(1 + \frac{1}{m}\right) \cdot f(m) \quad [7]$$

where σ_u=0 has been taken. Function Γ is tabulated and f(m) is a function of the Weibull modulus which depends on the geometry of loading. For example, for uniaxial tension f(m)=1, for three-point bending (Eq. 8):

$$f(m) = \left(2(m+1)^2\right)^{1/m} \quad [8]$$

and for four-point bending (Eq. 9):

$$f(m) = \left(\frac{4(m+1)^2}{m+2} \right)^{1/m} \quad [9]$$

Thus, the average fracture stress value, σ_{fm}, of a material with Weibull modulus, m, determined using a loading system other than uniaxial tension is related to the average value determined by using this last geometry, $\sigma_{uniaxial}$ (Eq. 10):

$$\sigma_{fm} = f(m) \cdot \sigma_{uniaxial} \quad [10]$$

The average strength values, σ_{fm1} and σ_{fm2} obtained for material volumes V_1 and V_2 are also related through the Weibull modulus (Eq. 11):

$$\frac{\sigma_1}{\sigma_2} = \left(\frac{V_2}{V_1} \right)^{1/m} \quad [11]$$

The results shown in Table I (21-23) confirm, at least qualitatively, the validity of equations [10-11].

Generally speaking, the simplest form of Weibull distribution can be used to characterize the fracture stress values of structural ceramic materials and, in fact, this simple form has been standardized in Europe (ENV-843-5). The probability of failure $P_f(\sigma)$ of a piece subjected to stress σ is given by (Eq. 12):

$$P_f(\sigma) = 1 - \exp\left(-\frac{\sigma^m}{\sigma_0^m} \right) \quad [12]$$

where m is the Weibull modulus and σ_0:

$$\sigma_0 = \frac{\sigma_{0V}}{V^{1/m}} \cdot f(m) \quad [13]$$

is the stress at which the probability of failure of the piece is of 63.2% and is generally called characteristic strength. This simple form of Weibull distribution assumes that there is no threshold stress below which fracture is not produced, which is appropriate to brittle materials such as ceramics.

To determine the values of the Weibull parameters in Eq. [5] on the basis of a series of experimental failure stress values, it is necessary to assume an estimator for the probability of failure. Among the different estimators proposed in the literature, the standard mentioned above requires the use of the estimator (Eq. 14):

$$P_f = \frac{n - 0.5}{N} \quad [14]$$

where N is the total number of pieces tested and n is the order number of the failure stress value considered, when these values are ordered on a rising scale.

The probability density associated with the distribution described by Eq. [12] is given by (Eq. 15):

$$p_f(\sigma) = \frac{m}{\sigma_0} \cdot \left(\frac{\sigma}{\sigma_0} \right)^{m-1} \cdot \exp\left(-\frac{\sigma^m}{\sigma_0^m} \right) \quad [15]$$

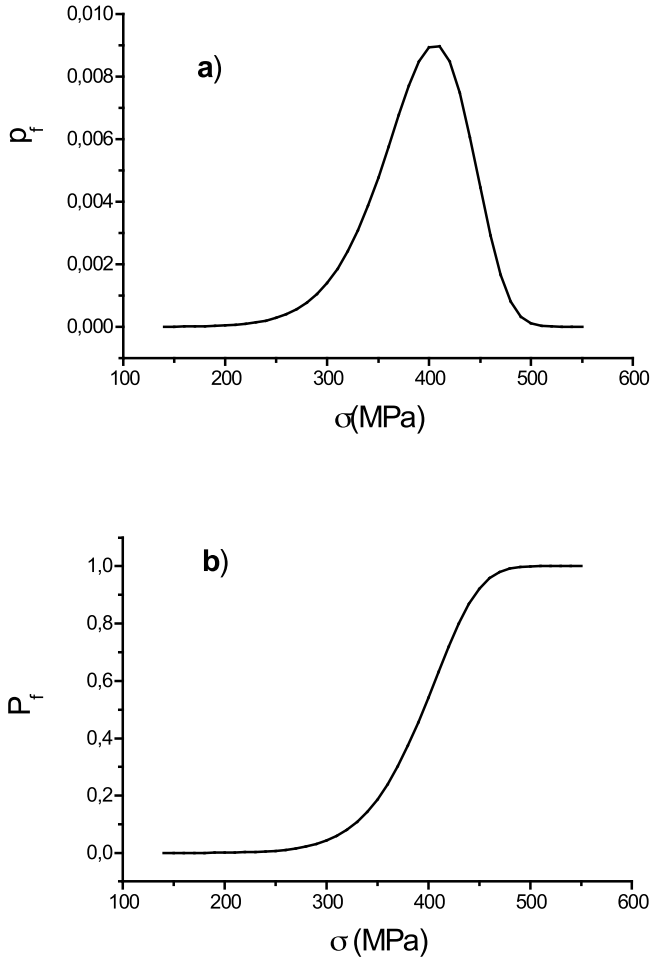

Fig. 6- Weibull distribution of strength values for a dense (99% of theoretical) and fine-grain (d_{50}≈2.2 μm) alumina material. Characteristic defects observed were pores developed from starting porosity in the green state such as that shown in Fig. 5. Weibull parameters (m=10, σ_0=410MPa) were calculated from 30 strength values of bar shaped specimens (3x4x50mm^3) tested in four points bending (spans 40-20mm), according to the European Standard ENV- 843-5.
a) Density of failure probability (p_f)
b) Cumulative failure probability (P_f)

To use the strength values of ceramic materials as design variables, parameters m and σ_0 are required and the fact that σ_u=0 must be taken into account. The width of the distribution of the strength values of materials is in correspondence with the Weibull modulus, m. Glasses, brittle materials par excellence, and traditional ceramic materials, such as refractory ceramics or ceramics for buildings, present very small Weibull modulus values (m≅1-2, 3-5, for glasses and traditional ceramic materials, respectively). The most common values for technical ceramics are m=5-22, where m=12-22 are relatively high values, found for example in commercial SiC (m=17-21) and Si_3N_4 (m=14-16) materials, with high-quality features and used in heavy-duty applications. In comparison, metals present values of m of over 30.

Figure 6 shows the Weibull distribution for the failure stress values of a dense (≅99% of the theoretical density) alumina with fine microstructure (average grain size = 2,2 μm). The Weibull distribution parameters (m=10, σ_0=410MPa) were calculated on the basis of 30 failure stress values for prismatic bars tested in four-point bending (bars: 3x4x50mm^3, distances between supports 40-20mm, ENV-843-5). The characteristic flaws found on the fracture surfaces of the beams of this material were pores developed from green body porosity, as that shown in Figure 5. The average strength calculated from of the experimental results and the value of $\Gamma(1+1/m)=\Gamma(1+1/10)$=0,9514 is 390MPa. According to equations [8-9] (f(10)=1.45, 1.73 for 4 and 3-point bending, respectively), if during the experiments beams of 3x4x40mm^3 of the material had been tested in uniaxial tension, the average strength value that would have been obtained (269MPa) would have been 30% lower and, if the tests had been done in three-point bending, with a distance of 40mm between supports, the average value obtained would have been 20% higher.

The failure probability density versus stress plot (Fig. 6a) clearly shows that the distribution is not symmetrical around a central value, as occurs with the distributions called central limit, such as the Gaussian; the Weibull function belongs to the group of the so called extreme value distributions. The probability density increases gently as the stress values increase until they draw near to the stress value for which the probability density is a maximum. For values above this stress, the probability density falls brusquely. On the basis of the cumulative distribution of the failure probability (Fig. 6b), it is possible to determine the failure probabilities of pieces under stresses which have not been determined experimentally. For example, there is a non-inexistent failure probability (≅10^{-3} %) at such low stresses as 140MPa and a significant failure probability (≅10 %) at 330MPa. From the values for the cumulative distribution of P_f it is possible to determine the stresses which condition the potential of the material for a particular application according to the safety factors required.

3. TOUGHENING MECHANISMS

The development of special microstructures which give rise to inelastic deformation processes during the fracture of ceramic materials and, thus, reduce their brittle behaviour, constitutes one of the main areas of research in new structural ceramic materials (4-6). A large number of monolithic ceramic composites constituted by ceramic matrices with dispersed second phases of different shapes have been developed and have constituted the basis of further developments. In particular, there is nowadays a great effort to design and fabricate ceramic materials following the so called biomimetic approach, which consists in fabricating hierarchical structures through artificial methods mimicking natural bio-structures, which in most of the cases present a failure behaviour that significantly overcome that of the individual components (26-27). In this sense, anisotropic materials on a macroscopic level have been developed (7,28-32). Materials formed by a combination of layers of different microstructures (7, 28-30) and materials fabricated by directional solidification of compositions close to eutectic ones (31-32) offer improved behaviour in comparison with the behaviour of monolithic materials with the same microstructure as that of the constituents. Another relatively new wide field of investigation, initially proposed by Niihara (33), is that of ceramic nanocomposites, materials with a dispersed second phase that exhibits a submicron and/or nanometric scale, and which show an increase of the strength and wear performance as compared to that exhibited by the matrix materials (33-34). The main concepts related to

toughening are discussed below for monolithic composites.

Inelastic deformation processes, called toughening mechanisms, produce dissipation of energy, reducing the elastic energy accumulated in the material at the start of fracture and/or contributing to delaying the growth of the crack during its propagation (6). In terms of the stress intensity factor, these mechanisms make it more difficult for the crack to advance because of a local reduction in the stress intensity at its front of it, since the microstructure of the material interacts directly with the crack or because internal stresses are developed tending to close the crack and opposing the external stresses.

In general, the stress-strain relationships when toughening mechanisms are operating are not linear up to the fracture, as occurs in the case of brittle materials. Figure 7 shows a load-displacement curve registered during the experiment on a material where toughening mechanisms contribute to its fracture (35). Initially, the material behaves in a linear manner until it reaches a load value from which point non-linear phenomena occur; the relative size of the linear and non-linear portions of the curves depend on the properties of the material and the toughening mechanisms in operation. This non-linear behaviour is also called apparently ductile, since it is not real ductility like that developed in metallic materials. Subsequently, once fracture has started, the action

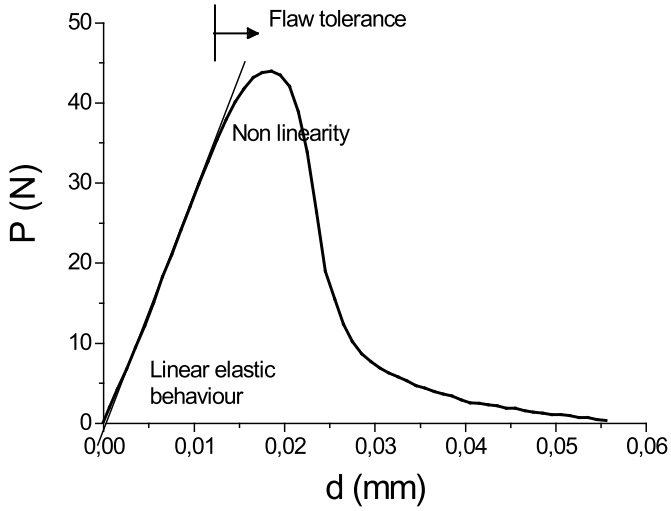

Fig. 7- General load (P)-displacement (d) relationship in materials in which toughening mechanisms are active. The curve corresponds to a material of alumina+10vol.% aluminium titanate tested in three points bending (35). At the start of loading the material behaves linearly and linearity is lost for higher loads.

of the toughening mechanisms can lead to an increase in the energy necessary to propagate the crack with its size (flaw tolerance).

Even though a large number of different toughened materials have been developed during the last years, the basic concepts for the classical toughening mechanisms in ceramic monolithic composites were already established at the 80´s, as summarised in the classical works by Freiman (36), Faber (37), Evans (6) and Steinbrech (5). It is possible to make several classifications of the toughening mechanisms considering the type of interaction existing between the material's microstructure and the crack and the mechanism's range of action (5,6,36-37). When the mechanism's extent of action is smaller or of the same order as the material's microstructure, they are called short-range mechanisms, while long-range mechanisms present larger extents of action (Table II). In practice, it is observed that several toughening mechanisms can act simultaneously (6,38), but the interactions between them are generally almost unknown and could produce both synergic effects, which increase toughness more than anticipated, and harmful effects (6).

TABLE II. TOUGHENING MECHANISMS IN CERAMICS. THE MAXIMUM VALUES OF THE CRITICAL STRESS INTENSITY FACTOR REACHED (K_∞)* AT THE STATIONARY STATE OF THE R CURVE FOR DIFFERENT MATERIALS ARE SHOWN (5,6,36-37).

Short-range		
Toughening mechanism	K_∞ MPa·m$^{1/2}$	Flaw tolerance
Crack bowing	2-4	No - Limited
Crack deflection	2-4	No - Limited
Long-range		
Toughening mechanism	K_∞ MPa·m$^{1/2}$	Flaw tolerance
Crack-shielding		
- Phase transformation	15-20	Yes
- Microcracking	~ 5	Limited
Crack-interaction		
- Crack bridging	5-15	Yes
- Debonding and pull-out	~ 30	Yes

*Values of K_∞ are shown for comparative purposes as absolute values may depend on testing method

3.1. Short-range mechanisms

Short-range mechanisms are produced when the interaction of the crack with the microstructure is limited to the crack tip. They lead to limited increases in toughness with crack extension (limited flaw tolerance) and, thus, the toughening effects may not be visible in standard tests for determining toughness using cracks with lengths longer than the size of the microstructure (Table II). The mechanisms of bowing the crack front and deflecting the crack's plane were identified. The crack is bowed when its front is stopped at several points due to the presence of inclusions of a second phase or heterogeneities of the matrix itself. The part of the crack front which is not held back continues to advance, which means that the crack front curves and, consequently, greater stress is required to propagate it. The increase in toughness produced while the crack is being bowed depends on the volumetric fraction of obstacles present, their shape and their toughness (37).

When deflection or diverting the plane of the crack occurs, the increase in toughness is due to the changes in orientation in the direction of crack propagation, which produces rough fracture surfaces, the opposite of the flat fracture surfaces exhibited by monocrystals. The deviation could consist of the turning or bending of the fracture plane from the original one, which implies that a fracture in Mode I becomes a combination of modes I, II and III (Fig. 1).

In the simplest case of single-phase polycrystalline materials, deflection of the crack may occur because the different grains present easy cleavage planes with different orientations. Moreover, the crack may deviate towards the grain boundaries, which, as was discussed before, are easy paths for propagation. Deviation of the crack can also be due to residual stresses which are developed in the materials that present thermal expansion anisotropy. In the case of materials composed of a matrix and a secondary phase, deflection of the

crack is determined by the characteristics of the boundaries between second phase grains and the matrix, which can be weak, constituting an easy path for propagation, and/or present localized residual stresses (37).

The effectiveness of crack deflection as a toughening mechanism depends on the shape of the particles which produce the deviation of the crack and on the density of their distribution, but not on their size, and is a maximum for particles with a disk-like shape or elongated bars. The increase in toughness which occurs could be as much as 100% with respect to the toughness of the same material with flat fracture (37).

3.2. Long-range mechanisms

Long-range mechanisms are processes which occur around the crack tip and surrounding the crack wake and may produce extensive flaw tolerance. There are two main groups among these mechanisms: crack-shielding mechanisms and crack interaction mechanisms (Table II).

In the crack-shielding mechanisms, irreversible processes are activated in the area surrounding the crack tip, which is known as the process zone, due to the stress field associated with the crack. These irreversible processes lead to microstructural changes that surround the crack wake as the crack propagates. They give rise to dilatation which is transmitted in the form of compressive forces on the crack lips while the crack propagates. The magnitude of these forces is determined by the stresses necessary to prevent the area where irreversible processes are developed from increasing in volume.

There are two irreversible processes that might be responsible for crack-shielding (6,37). On the one hand, there is a phenomenon well known in steels, the martensitic phase transformation induced by the stress field of a crack, which is accompanied by an increase in volume. In the case of ceramic materials, the most representative example is the transformation of zirconia from tetragonal phase to monoclinic phase. This phase transformation implies volumetric expansion of 3-5% and has been the subject of numerous studies which led to a new family of ceramic materials (5,6,37,39-40) with large increases in toughness (Table II). On the other hand, microcracking of materials surrounding the tip and on the wake of the main crack produces an increase in volume which leads to compressive forces on the crack which is being propagated, as occurs in the case of expansive transformation. Moreover, the microcracked zone presents a lower elastic modulus than the rest of the material, which also contributes to the effect of shielding of the main crack because of the reduction of the energy at the crack tip(6). A phenomenon that may occur associated with the formation of microcracks is the branching of the main crack, which creates an increase in volume equivalent to what occurs during microcracking (37).

The appearance of microcracks in the main crack's stress field is the result of local internal residual stresses which are present in the material. The origin of these residual stresses may be anisotropy in thermal expansion in monophase materials, the presence of secondary phases with different CTE from that of the matrix and/or phase transformation. The microcracks formed surround the grains when these are subjected to tension and are radial when the grains are subjected to compression.

The concept of critical grain size is crucial in designing materials toughened by microcracking. Thus, below a certain grain size, the microcracks do not open because of the effect of the main crack's stress field and toughening does not occur. Above a grain size known as critical size, spontaneous microcracking of the material occurs during cooling from sintering temperature, which can give rise to the general failure of the material. Moreover, in designing materials it must be remembered that the formation of microcracks may imply degradation in the material's resistance at the onset of fracture, before the process zone has been completely developed. This is because the effective size of the main crack increases due to its coalescence with the microcracks created at the crack tip (41).

In the modelling of crack-shielding mechanisms, the main parameters used to determine the increase in toughness are the density of elements which produce irreversible deformation, and the size and shape of the process zone (42-43). Generally speaking, the increase in toughness obtained by microcracking of the materials is considerably inferior to what can be achieved by means of the martensitic transformation of zirconia (37) (Table II).

In the other large group of long-range toughening mechanisms, crack interaction mechanisms (Table II), the increase in resistance to the propagation of cracks occurs as a result of the union of the fracture surfaces by means of microstructural objects, called ligaments (5,44). Thus, additional energy is required to separate the fracture surfaces (5,45). In general, the greater the crack opening displacement before the closing stress between the fracture surfaces is annulled, the greater the increase in toughness (5).

When the element acting as a ligament deforms elastically during the opening of the main crack until it breaks, the toughening mechanism is called the crack-bridging mechanism (Table II) and the increase in toughness is determined by fracture stress, the elastic modulus and the size of the ligament. A particular of this mechanism is based on the interlocking produced between the surfaces of the crack due to frictional sliding between grains on the intergranular fracture surfaces. In this case, rupture of the grains which produce this interlocking for the maximum opening of the crack does not occur; this has been described as particularly effective in alumina materials with large grain size (>40μm, 5,46-47). Toughening by crack-bridging is conditioned by the state of residual tensions of the particle and the matrix, since this determines whether the crack surrounds or draws nearer to the toughening ligament.

If, in addition to the effect of the union of the crack surfaces, the ligaments are debonded and pulled-out, the increase in toughness can be much greater (Table II). This contribution increases with the length of the ligaments and, consequently, is much more effective in the case of long fibres or single-crystal short fibres, when the matrix-fibre interface is relatively weak, and the crack is deflected on the matrix-fibre interface before the fibre is broken. This can occur at a relatively long distance from the main crack front (48).

4. MECHANICAL CHARACTERIZATION OF TOUGHENED MATERIALS

In materials whose behaviour cannot be regarded as brittle, the parameters deriving from linear elastic treatment to characterize fracture toughness, the critical stress intensity

factor, K_{IC}, and the critical energy release rate, G_{IC}, defined in 2.1, are not intrinsic properties, independent of the size of the crack and the loading system used to determine them experimentally (49-51). Thus, in this type of materials, specific treatment of fracture parameters is required.

The need for fracture criteria in regimes other than the linear elastic regime has led to the development of elastoplastic formulations that define more generalized parameters to characterize the behaviour of a crack in situations where plasticity occurs. Although these parameters were initially developed to study metallic materials, which present real ductility (52-54), they can be used in the field of ceramic materials where the aforementioned toughening mechanisms lead to apparently ductile behaviour. The mechanical parameters proposed to evaluate the fracture toughness of toughened ceramic materials are reviewed in which follows.

4.1. Fracture toughness

As Eftis et al. indicate (53-54), because of the mathematical complexity involved in dealing with inelastic and plastic phenomena, no analytical method for evaluating fracture toughness of semi-brittle and ductile materials can be regarded as having a universal application. Consequently, for each specific case (material type and application conditions), it would be necessary to evaluate which method gives the most reliable results. In order to solve this problem, one of the proposals is to extend the principles of linear elastic fracture to situations where the inelastic deformation occurs prior to fracture, so that fracture toughness can be determined. Parameters like resistance to crack growth, R curve, and J integral arise from this approach.

The R curve has been extensively used to characterize the fracture toughness of ceramic materials in which long-range toughening mechanisms are operative (49,55). On the R curve, the values of the parameters of linear elastic fracture mechanics (the critical energy release rate, G_{IC}, or the critical stress intensity factor, K_{IC}) are represented as a function of crack size. K_{IC} and G_{IC} are determined in standard tests, conducted with long cracks. Materials where long-range toughening mechanisms act show rising R curves, as a result of the activation of the different mechanisms as the cracks grows, until it reaches a stationary state (K_{∞} or G_{∞}); from this point no new contributions are made to the increase in toughness. The maximum value of toughness reached does not only depend on the materials, but also on the loading system, the size of the crack and its history prior to propagation (46,49,55-56)

When only short-range mechanisms act, toughness is determined by the details of the microstructure ahead the crack tip. As the crack grows, it intercepts different grains and grain boundaries, with different orientations from those on the original crack plane, and this implies that toughness also increases with the size of the crack until it reaches the value corresponding to the polycrystalline material. From this moment, the crack can be treated macroscopically as if it were propagating in a homogenous and isotropous body. Thus, the R curve behaviour occurs at the microstructural level and this is not detected in standard tests for determining toughness using long cracks (5,6).

It has been observed that the R curve behaviour determined in tests with long cracks can be different from the type of propagation of the natural flaws present in the same materials in normal working conditions since, in many cases, the high values of toughness of the stationary state reached during testing are not achieved. Small defects in the material can produce the catastrophic failure, without the process zone responsible for the greater toughness for long cracks being developed (5,36). For this reason, Steinbrech (5) proposed to carry out studies on R curve behaviour regarding the propagation of natural flaws. However, perhaps because of the experimental difficulty associated with the large number of tests this last type of characterization would involve, the majority of R curves for ceramic materials are constructed on the basis of results from tests performed with long cracks (6,49). Moreover, the form of the R curve may be affected by the geometry of the beam, especially in the case of materials with a high degree of plasticity (49-50,56).

The J-integral concept, formulated by Rice (57) quantifies the total energy produced by the stress and deformations in the neighbourhood of the crack tip, where a large part of the plasticity phenomena occur in the case of metals and a large part of the inelastic energy dissipation phenomena occur in ceramic materials where toughening mechanisms operate. These mechanisms produce the non-linear zone on the stress-strain curve (Fig. 7). The J-integral can be regarded as a generalization of the energy release rate, G, for fracture processes where the plasticity at the crack tip is notable. A critical value, J_{IC} in Mode I, is defined at the start of the propagation of the crack, which is in principle independent of its size and only depends on the material and its state of deformation. Thus, this concept is equivalent to the G_{IC} concept for linear and elastic materials.

The J_{IC} parameter, whose use is scant in the field of ceramic materials and restricted to materials with marked non-linear behaviour, such as refractories or graphite ceramics (58-59), seems to be suitable for characterizing fracture toughness when operating toughness mechanisms act over a short-range or long-range with limited R curve behaviour (60).

Eftis et al (53-54), Sakai et al. (59) and Gogotsi et al. (61) proposed the total energy of the crack propagation as being equal to the addition of an elastic component and another irreversible component which includes the contribution of non-linear phenomena. In this way, it is possible to use parameters based on the comparison of the mechanical response of the non-elastic materials with the response of a perfectly elastic linear material (59,61). It is possible then to define non-linear fracture toughness based on a macroscopic energy balance which includes total energy (53-54).

Numerous models are currently being developed to characterize the fracture of non-linear materials which take into account the influence of the zone surrounding the crack tip, in which the toughening mechanisms occur, avoiding the consideration of the singularities at the crack tip which considers the Linear Elastic Fracture Mechanics (62). For modelling purposes, the toughening processes are represented by means of a cohesive force which opposes the external stresses applied and is distributed on the surfaces of the crack. The most commonly used models are cohesive crack models, which assume that the crack is capable of transmitting stresses between its surfaces in accordance with a function that relates these stresses to the crack opening displacement. This function is known as the softening function and is an intrinsic characteristic of each material. The biggest limitation of these models is their complexity in terms of calculation (62).

4.2. Work of fracture

Unlike fracture toughness, the work of fracture, γ_{WOF}, is defined as the average value of external work consumed to produce a crack unit during quasi-static fracture. Experimentally, it is determined on the basis of area under the load – displacement of the load point curve, obtained during stable tests, where all the work done produces new fracture surfaces (63-65). The work done is divided by the projected area of the two fracture surfaces, which means that work of fracture is an average value for the entire fracture process. The advantage related to this energy parameter is that it does not require any assumptions about the constitutive equation of the body with the crack to discuss its propagation (59). Thus, it can be used to describe behaviours which are separate from linearity and it is an additive parameter which makes it possible to quantify the different contributions to energy dissipation during fracture (43,65-67).

Although work of fracture has been successfully used to describe the fracture of refractories (58), its use in advanced ceramic materials has been much more limited (35,63,65,68), due to the experimental difficulty involved in obtaining stable tests in low-toughness materials. Thus, even in the case of such widely studied and characterized materials as dense single-phase aluminas, the majority of the work of fracture experiments described in scientific literature refers to materials with average grain sizes of over 5 μm (69-70). Recently (35) an alumina material with a smaller average grain size (3.5μm) was characterized, giving a work of fracture value of 10J/m^2. Although this value is significantly lower than the value of materials with coarser microstructures (35,70) (e.g: 20J/m^2 for an alumina with an average size of 5.5μm (35)), it is still much higher than the value ($\cong$6 J/m^2) determined for the preferred cleavage plane in alumina single-crystals (71), due to the above mentioned processes associated with the fracture of polycrystals.

5. DETERMINATION OF FRACTURE PARAMETERS

There is a wide variety of tests to determine the mechanical parameters of ceramics. Indentation experiments constitute a family of widely-used techniques to evaluate some properties such as fracture toughness (72-73). Moreover, the general relationship between contact stiffness, the area of contact and the elastic properties of the materials has led to instrumented indentation being a fundamental tool for the mechanical characterization of materials (74-75). However, this family of techniques will not be considered in this work since the study of them would require specific treatment and a particular in-depth discussion.

To determine the fracture behaviour of ceramics, specimens with cracks of known geometry and size are subjected to increasing deformations. When unstable fracture conditions are used, it is not possible to ensure that the work done on the specimen transforms exclusively in new fracture surfaces. Thus, they are not valid for determining the work of fracture (63-65). Besides, these types of conditions can give fracture toughness values that are higher than the actual values (76). For this reason, the use of stable tests, where the growth of the crack takes place in a controlled manner, is considered to be more appropriate for determining all the fracture parameters.

There is a wide variety of specimen and load geometries where the stress intensity factor is known for a crack of a given shape and size (77-82). Due to the difficulties involved in machining ceramic parts with special shapes as well as to the tendency of brittle materials to fail under shear stresses originated by deficient clamping and/or alignment, the most widely used geometry for mechanical testing of ceramics is that of parallelepipedic bars subjected to bending, due to the ease mechanization and the simplicity of the test apparatus required.

The stability of a fracture test is determined by the geometry and testing conditions as well as by the mechanical and elastic properties of the material. According to the stability analysis conducted by Bar-On et al. (76) on pre-cracked parallelepipedic beams in three-point bending experiments, which are more stable than four-point tests (83), the parameters which determine that the test is stable in a material, in the absence of an R curve, are: the dimensions of the beam, the crack size, the distance between supports, the compliance of the beam and the compliance of the set of supports and test machine. These authors established the theoretical relations between the parameters, which make it possible to determine the conditions that produce stable tests.

The two testing variables that can be easily controlled during mechanical testing are load and displacement of the loading frame. Tests are performed by using a monotonous rising ramp of one of these parameters. At the onset of failure, both parameters experience a decrease and thus, the response of the loading machine to follow the imposed ramp would provide extra energy to the sample leading to unstable fracture of materials that do not present R curve. As shown by Pastor et al (68, 78) the choice of a test variable that increases monotonically during the whole test, such as the crack mouth opening displacement (CMOD), is much more convenient to reach stability when testing ceramics. Main problem of CMOD is the difficulty involved in detecting and monitoring such parameter, therefore, displacement control is preferred.

The generation of suitable cracks is a fundamental requirement for the validity of the tests. In this respect, the generation of cracks starting from indentations or notches, subjected to compression (SEPB: Single Edge Precracked Beam) was proposed. This technique involves great difficulty as regards controlling the size of the crack generated and ensuring that the beams, made of brittle materials, do not break when the crack is being introduced (78).

The introduction of straight notches by means of cutting processes is an alternative to generate cracks. According to the reviews conducted by different authors (79-82), the experiments with beams in bending with straight notches (SENB: Single Edge Notch Beam, Fig. 8a) lead to critical stress intensity factor values which are highly reproducible when results between different laboratories are compared. In addition, they are easy to produce, as compared to the complexity of preparing other notch geometries such as Chevron, and the analysis of the results obtained is simple, in comparison with the results from other configurations, such as double torsion (9). The main drawback of the SENB tests is the dependence of the results on the radius of the notch, since its behaviour becomes more remote from the behaviour of a crack as its radius increases (79).

The general recommendation for obtaining constant values for the critical stress intensity factor of structural ceramic materials, which do not depend on the radius of the notch and are comparable with those obtained on the basis of cracks, using the SENB method (81), is to make notches with a radius

of less than 10 μm. However, it has been observed that the actual value of the radius below which constant values are reached depends on the microstructure and type of material (79). In alumina materials, constant toughness values are obtained for radii smaller than approximately three times the grain size or the size of the characteristic flaws (pores, microcracks, machining damage, etc.) (79). For these reasons, SENB method is not considered for European (CEN) and ISO standards.

As an alternative to the use of notched beams with curved notch tips, the use of Single Edge V Notched Beams (SEVNB) has been proposed. In these specimens, the curved notch tips are corrected with a razor blade and diamond paste to reduce their radius (Fig. 8b). In this case, notch tips in a V-shape are obtained. As can be observed on the fracture surface in Fig. 9, the fracture starts in the area of wear the diamond produces in the grains.

The values of the mechanical parameters can vary significantly depending on both the test conditions and

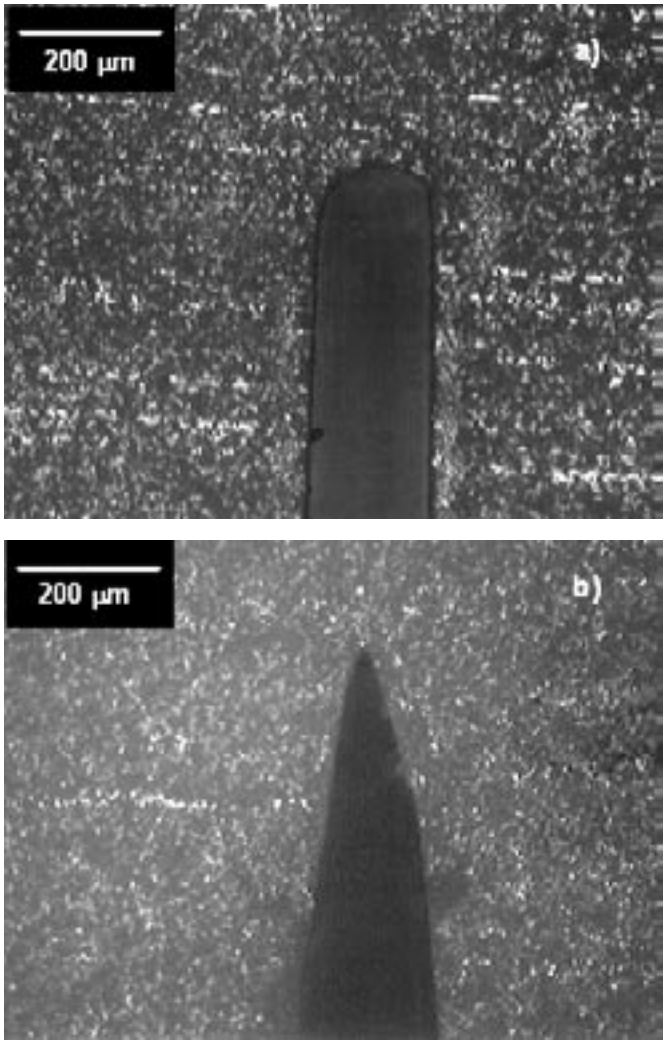

Fig. 8- Characteristic straight notches in structural ceramics. Specimen of dense (99% of theoretical) and fine-grain (d_{50}≈2.2 μm) alumina sintered at 1450ºC. Optical microscopy micrographs.
a) SENB: Notch introduced with a thin (150 μm) diamond disc.
b) SEVNB: Notch introduced with a thin (150 μm) diamond disc and subsequently corrected with a razor blade with diamond past (15, 6 and 1 μm, successively) to reduce the tip radius. The V shaped tip is observed (85).

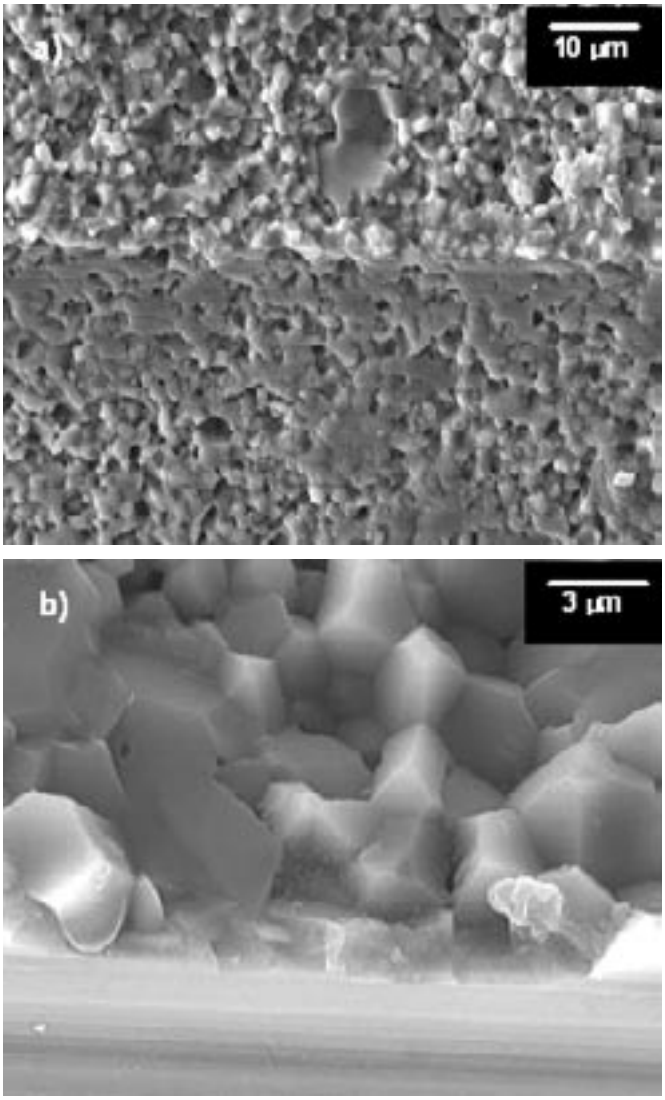

Fig. 9- Characteristic fracture surfaces of SENVB specimens. Specimen of dense (99% of theoretical) and medium-grained (d_{50}≈5.5 μm) alumina sintered at 1550ºC. (85). The area for the start of fracture at the notch tip is shown at the bottom of the micrographs obtained by scanning electron microscopy.

the characteristics of the notches introduced. For example, the value of the critical stress intensity factor in Mode I corresponding to dense alumina materials (>98% of theoretical density) of fine grain (<5 μm) range between ≅4.5 MPa·m$^{1/2}$ for unstable tests and notch radii of around 100μm (Fig. 8a) (18,79,84) and ≅2.9 MPa·m$^{1/2}$ for stable SEVNB beams, with notch radii of below 20μm (Fig. 8b) (85).

There are numerous expressions which make it possible to calculate the Mode I critical stress intensity factor in bending tests, starting from the test load and the geometry of the notched beam. Guinea et al. (86) proposed the use of the following equation (Eq. 16):

$$K_I = \frac{3 \cdot P \cdot L}{2 \cdot B \cdot W^{3/2}} \cdot Y(\alpha) \qquad [16]$$

where P is the load applied, L is the span, B and W are the width and the height of the beam, respectively, and Y(α) is a geometrical factor that depends on the normalized notch

length, α=a/W, where a is the depth of the notch (Eq. 17):

$$Y(\alpha) = \frac{\sqrt{\alpha}\cdot(1.99 + F(\alpha) + 4\cdot(W/L)\cdot(-0,09 + H(\alpha)))}{(1-\alpha)^{3/2}\cdot(1+3\alpha)}$$

[17]

where:

$$F(\alpha) = 0.83\cdot\alpha - 0.31\cdot\alpha^2 + 0.14\cdot\alpha^3$$

[17a]

and:

$$H(\alpha) = -0.42\cdot\alpha + 0.82\cdot\alpha^2 - 0.31\cdot\alpha^3$$

[17b]

This expression is valid, for any value of a, and parallelepipedic beams in three-point bending with a relation between the span and the height of the beam, β=L/W, greater than 2.5.

The other parameter of linear elastic fracture described in 2.1, the critical energy release rate (G_{IC}), is calculated on the basis of the critical stress intensity factor and the material's Young´s modulus according to Irwin's classical relationship (Eq. 4).

The work of fracture (γ_{WOF}, section 3) of notch beams subjected to bending is calculated as the area under the load-displacement of the load point curve divided by double the transversal section of the initial un-notched part of the beam, (W-a)·B, where W, B and a have the same meaning as in Eq. [16].

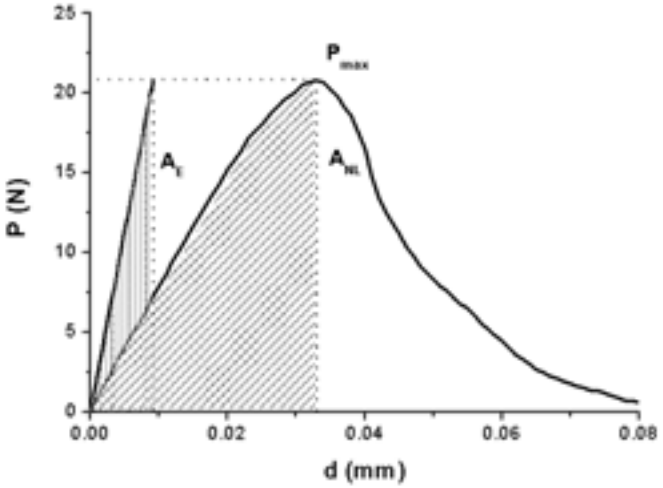

Fig. 10- Representation of the procedure followed to calculate the critical J-integral value, J_{IC}, (58). The curve corresponds to a material of alumina+40vol.% aluminium titanate tested in three points bending. A_{NL} and A_E are the areas under the load-displacement curves of specimens tested with a notch and unnotched specimens, respectively. The unnotched specimens were tested only up to 5 N and the obtained load-displacement slope was prolonged to the maximum load of the notched specimen.

There are different methods for calculating the critical J-integral value, J_{IC}, (58,87-88). The majority of them are based on the calculation of the energy absorbed by pre-cracked specimens, determined on the basis of the area under the load – crack opening displacement curves (87). The J-integral values can also be evaluated on the basis of the load–displacement of the load point curves of two tests conducted on specimens with different crack lengths (88). The two methods require identification of the crack which is propagated. Alternatively, Bradt et al. (58) proposed a method for refractory materials with marked non-linear behaviour. The method is based on the difference in areas between the load-displacement curve of an un-notched specimen of the material, where linear elastic behaviour is assumed, and the load-displacement curve of a notched specimen of the same material, which presents non-linear behaviour (Fig. 10) (35). On the basis of the difference in areas, the value of J_{IC} is calculated using Eq. [18].

$$J_{IC} = \frac{2}{(W-a)\cdot B}\cdot\int_0^{\delta_J} P\cdot d\delta = \frac{2}{(W-a)\cdot B}\cdot(A_{NL} - A_E) = \frac{2}{(W-a)\cdot B}\cdot A_J$$

[18]

where A_{NL}, A_E and A_J refer to the area under the curve for load (P) – displacement (δ) (to the maximum load point) in the test of notched specimen, of the un-notched specimen (up to the same maximum load value) and to the difference between the two areas respectively. W, B and a have the same meaning as in Eq. [16]. For materials which present real or apparent ductility, the fracture toughness value, J_{IC}, thus obtained is higher than the critical energy release rate (G_{IC}) (35,58) and corresponds to that of the component or structure of the same material whose integrity is analyzed if it is in the same deformation state as the beam tested.

The load-displacement curves of the controlled fracture tests also make it possible to determine a material's R curve behaviour. In principle, as the toughness and length of the crack must be known at each point of the R curve, the crack must be measured constantly throughout the experiment.

It is not always possible to determine the crack length at every moment of the test, especially for materials constituted by phases with large differences in hardness and in which residual stresses are present (35). The low-quality of polished surfaces of specimens of such materials makes enormously difficult the identification and monitoring of the propagating crack and thus, the "in situ" measurement of crack length.

An alternative is to calculate the R curve by defining an equivalent crack length assuming linear elastic behaviour for the material, as was proposed by Eftis et al. (53-54). To do this, it is necessary to know the relationship between the increase of compliance, C, which the specimen experiences when the crack is growing, and the length of the same (51,89-91). Guinea et al. (86) proposed the following expression (Eq. 19):

$$\alpha = \frac{(C\cdot E'\cdot B)^{1/2}}{\left[C\cdot E'\cdot B + q_1\cdot(C\cdot E'\cdot B)^{1/2} + q_2\cdot(C\cdot E'\cdot B)^{1/3} + q_3\right]^{1/2}}$$

[19]

where α=a/W is the normalized notch length, E' is the generalized elastic modulus: equal to the Young`s modulus, E, for plane stress and $E/(1-\upsilon^2)$ for plane strain (υ is the Poisson coefficient), B has the same meaning as in Eq. [16] and q_i are constants which depend on the relationship between the span and the height of the beam, β=L/W. This expression is valid in the range $2.5 \le \beta \le 16$.

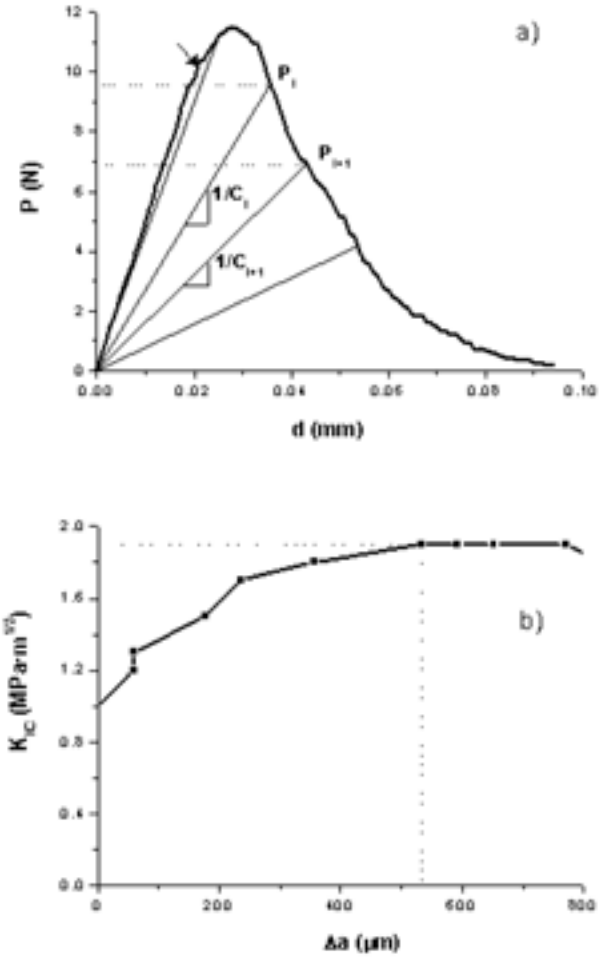

Fig. 11- Indirect procedure followed for R curve construction by estimating the crack length from the compliance change of the specimen (35). The curves correspond to a notched specimen of alumina+40vol.% aluminium titanate tested in three points bending.
a) Characteristic load – displacement curves. The arrow marks the point where the non-linear behaviour starts and that is selected to determine the onset of crack propagation. From this point, the increments in the crack length ($\Delta a=a_{i+1}-a_i$) would produce the changes in the compliance (C_i, C_{i+1}).
b) Characteristic R curve where an increase of the critical stress intensity factor is observed for increasing crack sizes up to a stationary value (K_∞).

As Fig. 11 shows, the procedure for determining the growth of the crack (Δa) and constructing the R curve requires knowing the point on the load-displacement curve where the crack begins to be propagated. The most widely used criterion establishes the start of the fracture on the load-displacement curve where linearity is lost when the materials are being loaded (indicated with an arrow in Fig. 11a) (51,92).

As from this point, the increases in the length of the crack ($\Delta a=a_{i+1}-a_i$) produce an increase in the compliance of the beam (C_i, C_{i+1}, Fig. 11a). The values of the critical stress intensity factor (K_{IC}), for each crack length and for the corresponding load value on the load-displacement curve are determined in the conventional manner proposed for this parameter, by using, for example, the equation indicated earlier (Eq. 16).

An R curve which presents upward behaviour until it reaches a stationary value of K_{IC} (K_∞, Fig. 11b), reveals the increase in toughness with crack extension (flaw tolerance) on a crack length, Δa_∞, associated with the development of a process zone where toughening mechanisms are in operation.

It is important to point out that, although this indirect method of constructing the R curve is very useful for materials where it is difficult to monitor the crack during the test, it can lead to over dimensioning of the size of the process zone developed in cases where the stiffness of the material diminishes due to microcracking processes, since the method implies the increase of compliance being exclusively associated with crack size. In these cases, the proposal has been to combine the determination of the R curve with the determination of other mechanical parameters such as J_{IC} for the complete analysis of the mechanical behaviour of materials (35).

6. FINAL CONSIDERATIONS

The strength of ceramic materials is an extremely variable parameter, which depends on the distribution of defects present in their interior. Thus, the characterization of a material on the basis of this parameter requires the determination of the distribution of strength values so that the probability of failure under the stress levels required for each application can be forecast.

Analysis of the processes which contribute to the fracture of ceramic materials is essential for designing new materials for structural applications. The fracture toughness is defined as an intrinsic property of the material, which is dependent on the microstructure and independent of the particular distribution of flaws. The two basic Linear Elastic Fracture Mechanics toughness parameters, the critical stress intensity factor, K_{IC}, and the critical energy release rate, G_{IC}, have been discussed.

The concept of fracture toughness has made it possible to design new microstructures which produce toughening mechanisms during fracture of the materials. These mechanisms can give flaw-tolerant materials, due to an increase in resistance to the propagation of the crack with its size, named R curve behaviour. The resulting material strengths depend on the details of the resistance curve and the initial crack lengths, such that toughness and strength optimization usually involve different choices of microstructure.

The levels of inelastic deformation reached in ceramic materials in which toughening mechanisms operate can restrict the direct utilization of the condition of brittle fracture and, thus, limit the concept of fracture toughness as an intrinsic parameter of the material.

The mechanical characterization of the materials which deviate from brittle behaviour is still under discussion. In this work, three parameters which provide different information about the magnitude of the toughening reached at each stage of fracture were analyzed. The fracture criterion based on the J integral, J_{IC}, makes it possible to determine the fracture toughness at the onset of crack propagation when the application of brittle fracture criteria would lead to lower fracture toughness values. The R curve makes it possible to establish and quantify the increase in toughness produced when a process zone develops at the crack tip and remains surrounding the crack wake during crack propagation. The work of fracture, γ_{WOF}, is an average value for the entire fracture process, which evaluates the contribution of all the toughening mechanisms. Since it is an additive parameter,

it would be suitable for characterizing macroscopically anisotropic materials, as is the case of materials formed by the combination of different microstructures ordered with a preferential orientation such as laminates.

To identify the toughening mechanisms operating in the materials, acting at the onset of crack propagation in a frontal process zone or on the wake of the same when propagation takes place, it will be necessary to combine joint analysis of the parameters, J_{IC} –onset- and R curve –propagation-, with microstructural and fractographic observations.

ACKNOWLEDGEMENTS

The financial support of the Projects CICYT MAT2003-00836 and MAT2006-13480 C02-01 and the Postdoctoral Fellowship MEC EX-2006-0555 (Spain) is acknowledged.

REFERENCES

1. R.J. Brook. "Advanced Ceramic Materials: An Overview", p. 1-8 in Concise Encyclopedia of Advanced Ceramic Materials. Ed. R. J. Brook, R. W. Cahn, M. B. Bever, Pergamon Press, Oxford (UK) 1991.
2. R.W. Davidge, A.G. Evans. "The Strength of Ceramics". Mater. Sci. Eng. 6 281-298 (1970).
3. R.W. Davidge, "The Fracture Strength of Ceramics", p. 75-103 in Mechanical Behaviour of Ceramics. Ed. R. W. Cahn, M. W. Thompson, I. M. Ward, Cambridge University Press, Cambridge (UK) 1979.
4. M.P. Harmer, H.M. Chan, G.A. Miller. "Unique Opportunities for Microstructural Engineering with Duplex and Laminar Ceramic Composites". J. Am. Ceram. Soc. 75 [7] 1715-28 (1992).
5. R.W. Steinbrech. "Toughening Mechanisms for Ceramic Materials". J. Eur. Ceram. Soc. 10 131-142 (1992).
6. A.G. Evans. "Perspective on the Development of High-Toughness Ceramics". J. Am. Ceram. Soc. 73 [2] 187-206 (1990).
7. S. Bueno, C. Baudin. "Flaw Tolerant Ceramic Laminates with Negligible Residual Stresses between Layers". Key Eng. Mater. 333 17-26 (2006).
8. D. Casellas, M.M. Nagl, M. Vélez, M. Anglada. "Determinación de la presencia de fatiga mecánica en materiales cerámicos". Bol. Soc. Esp. Ceram. V., 38 [2] 101-110 (1999).
9. A.H. de Aza, Y.J. Chevalier. "Revisión de la técnica de doble torsion y del método experimental en materiales cerámicos". Bol. Soc. Esp. Ceram. V., 40 [2] 93-99 (2001).
10. C. Baudín. "Thermal shock resistance of refractories. I: "Resistencia de los refractarios al choque térmico I: aproximación termoelástica y criterio de balance energético". Bol. Soc. Esp. Ceram. V., 32 [4] 237-244 (1993).
11. C. Baudín. "Resistencia de los refractarios al choque térmico II: Teoría unificada de Hasselman". Bol. Soc. Esp. Ceram. V., 32 [5] 293-298 (1993).
12. K. Adachi, K. Kato, N. Chen. "Wear map of ceramics". Wear 203-204, 291-301 (1997)
13. I.M. Hutchings. "TRIBOLOGY: Friction and Wear of Engineering Materials". Ed. Edward Arnold, Hodder Headline PLC, London (UK) 1992.
14. R. Torrecillas, J.S. Moya, "Mecánica de fractura en materiales cerámicos frágiles. I: Principios fundamentales". Bol. Soc. Esp. Ceram. V., 27 [3] 123-135 (1988).
15. R. Torrecillas, J.S. Moya. "Mecánica de fractura en materiales cerámicos frágiles. II. Propagación subcrítica de grietas". Bol. Soc. Esp. Ceram. V., 28 [4] 275-283 (1989).
16. J. A. Rescalvo. "Principios de la mecánica de la fractura". Rev. Metal. CENIM, 17 [2] 93-96 (1981).
17. A.A. Griffith. "The Phenomena of Rupture and Flow in Solids". Phil. Trans. Roy. Soc. London A, 221 163-198 (1921).
18. R.W. Rice, S.W. Freiman, P.F. Becher. "Grain-Size Dependence of Fracture Energy in Ceramics: I, Experiment". J. Am. Ceram. Soc. 64 [6] 345-350 (1981).
19. G.R. Irwin. "Fracture", p. 551-589 in Encyclopaedia of Physics. Ed. S. Flüge, Springer Verlag, Berlin (Germany) 1958.
20. R. Morrel. "Fractography of Brittle Materials". Measurement Good Practice No. 15. The National Physical Laboratory, Teddington, Middlesex (UK) 1999.
21. Y. Katayama, Y. Hattori. "Effects of Specimen Size on Strength of Sintered Silicon Nitride". J. Am. Ceram. Soc. 65 [10] C164-C165 (1982).
22. T.T. Shih, J. Opoku. "Application of fracture mechanics to ceramic materials - State of the art review". Eng. Fract. Mech. 12 [4] 479-498 (1979).
23. D.W. Richerson. "Mechanical Behavior and its Measurement". p. 162-203 in Modern Ceramic Engineering: Properties, Processing and Use in Design. Second edition. Marcel Dekker Inc., New York (USA) 1992.
24. W. Weibull. "A Statistical Distribution Function of Wide Applicability". J. Appl. Mech. 18 [3] 293-97 (1951).
25. K. Trustum, A.S. Jayatilaka. "On the estimating of the Weibull modulus for a brittle material". J. Mater. Sci. 14 1080-1084 (1979).
26. I. A. Aksay, D. M. Dabbs, J. T. Staley, M. Sarikaya. "Bioinspired processing of ceramic-matrix composites". p. 1-14 in "Ceramics toward the 21st century", Ed. N. Soga, A. Kato. The Ceramic Society of Japan, Tokyo (Japan) 1991.
27. G. Mayer. "New classes of tough composites materials – Lessons from natural rigid biological systems". Mat. Sci. Eng. C – Bio. S. 26 1261-1268 (2006).
28. J. Gurauskis, A.J. Sánchez-Herencia, C. Baudín. "Alumina-zirconia layered ceramics fabricated by stacking water processed green ceramic tapes". J. Eur. Ceram. Soc. 27 [2-3] 1389-1394 (2007).
29. R. Bermejo, A.J. Sanchez-Herencia, C. Baudin, L. Llanes. "Residual stresses in Al_2O_3-ZrO_2 multilayered ceramics: nature, evaluation and influence on the structural integrity".Bol. Soc. Esp. Ceram. V., 45 [5] 352-357 (2006).
30. T. Lube, J. Pascual, F. Chalvet, G. de Portu. "Effective fracture toughness in Al_2O_3–Al_2O_3/ZrO_2 laminates". J. Eur. Ceram. Soc. 27 [2-3] 1449-1453 (2006).
31. J. Llorca J, V.M. Orera, "Directionally solidified eutectic ceramic oxides". Prog. Mater. Sci., 51 [6] 711-809 (2006).
32. C. Baudín, A. Sayir, M.H. Berger. "Mechanical behaviour of directionally solidified alumina/aluminium titanate ceramics". Acta Mater. 54 3835-3841 (2006).
33. K. Niihara. "New design concept of structural ceramics - ceramic nanocomposites". J. Ceram. Soc. Jpn. 99 [10] 974-982 (1991).
34. S. Choi, H. Awaji. "Nanocomposites – a new material design concept". Science and Technology of Advanced Materials. 6 2-10 (2005).
35. S. Bueno, M.H. Berger, R. Moreno, C. Baudín. "Fracture behaviour of microcrack – free alumina / aluminium titanate ceramics with second phase nanoparticles at alumina grain boundaries". J. Am. Ceram. Soc. To be published.
36. S.W. Freiman. "Brittle Fracture Behaviour of Ceramics". Ceram. Bull. 67 [2] 392-402 (1988).
37. K.T. Faber. "Toughening Mechanisms for Ceramics in Automotive Applications". Ceram. Eng. Sci. Proc. 5 [5-6] 408-439 (1984).
38. J. Rödel. "Interaction Between Crack Deflection and Crack Bridging". J. Eur. Ceram. Soc. 10 143-150 (1992).
39. M.I. Osendi, J.S. Moya. "Fundamentos de la transformación martensítica. Su importancia en el diseño de futuros materiales cerámicos". Bol. Soc. Esp. Ceram. V., 21 [1] 33-40 (1982).
40. P.M. Kelly, L.R.F. Rose. "The martensitic transformation in ceramics - its role in transformation toughening". Prog. Mater. Sci. 47 [5] 463-557 (2002).
41. L.R.F. Rose. "Effective Fracture Toughness of Microcracked Materials". J. Am. Ceram. Soc. 69 [3] 212-14 (1986).
42. A.G. Evans, K.T. Faber. "Toughening of Ceramics by Circumferential microcracking". J. Am. Ceram. Soc. 64 [7] 394-398 (1981).
43. A.G. Evans, K.T. Faber. "Crack-Growth Resistance of Microcracking Brittle Materials". J. Am. Ceram. Soc. 67 [4] 255-260 (1984).
44. P.F. Becher. "Microstructural Design of Toughened Ceramics". J. Am. Ceram. Soc. 74 [2] 255-69 (1991).
45. J. Rödel. "Crack Closure Forces in Ceramics: Characterization and Formation". J. Eur. Ceram. Soc. 9 323-334 (1992).
46. R. Knehans, R.W. Steinbrech. "Memory effect of crack resistance during slow crack growth in notched Al_2O_3 bend specimens". J. Mater. Sci. Lett. 1 327-329 (1982).
47. P.L. Swanson, C.J. Fairbanks, B.R. Lawn, Y. Mai, B.J. Hockey. "Crack-Interface Grain Bridging as a Fracture Resistance Mechanism in Ceramics: I, Experimental Study on Alumina". J. Am. Ceram. Soc. 70 [4] 279-289 (1987).
48. P. Miranzo, J.S. Moya. "Reforzamiento de materiales cerámicos y vítreos por fibras". Bol. Soc. Esp. Ceram. V., 27 [3] 145-151 (1988).
49. R.W. Steinbrech, A. Reichl, W. Schaarwächter. "R-Curve Behavior of Long Cracks in Alumina". J. Am. Ceram. Soc. 73 [7] 2009-2015 (1990).
50. H.L. Ewalds, R.J.H. Wanhill. "Stable Crack Growth and the R-Curve Concept", p. 86-94 in Fracture Mechanics. Edward Arnold (Publishers) Ltd., London (UK) 1984.
51. M. Sakai, J. Yoshimura, Y. Goto, M. Inagaki. "R-Curve Behaviour of a Polycrystalline Graphite: Microcracking and Grain Bridging in the Wake Region". J. Am. Ceram. Soc. 71 [8] 609-16 (1988).
52. J.A. Rescalvo. "Mecánica de la fractura elasto-plástica". Rev. Metal. CENIM. 18 [2] 91-96 (1982).
53. J. Eftis, H. Liebowitz. "On fracture toughness evaluation for semi-brittle fracture". Eng. Fract. Mech. 7 101-135 (1975).
54. J. Eftis, D.L. Jones, H. Liebowitz. "On Fracture Toughness in the nonlinear range". Eng. Fract. Mech. 7 491-503 (1975).
55. E. H. Lutz, N. Claussen, M. V. Swain. "K^R-Curve Behavior of Duplex Ceramics". J. Am. Ceram. Soc. 74 [1] 11-18 (1991).
56. T. Fett, D. Munz, R. D. Geraghty, K. W. White. "Influence of specimen geometry and relative crack size on the R-curve". Eng. Fract. Mech. 66 [4] 375-386 (2000).

57. J.R. Rice. "A Path Independent Integral and the Approximate Analysis of Strain Concentration by Notches and Cracks". J. Appl. Mech. 35 379-386 (1968).
58. J. Homeny, T. Darroudi, R.C. Bradt. "J-Integral Measurements of the Fracture of 50% Alumina Refractories". J. Am. Ceram. Soc. 63 [5-6] 326-331 (1980).
59. M. Sakai, K. Urashima, M. Inagaki. "Energy Principle of Elastic-Plastic Fracture and Its Application to the Fracture Mechanics of a Polycristalline Graphite". J. Am. Ceram. Soc. 66 [12] 868-874 (1983).
60. R. N. Stevens, F. Guiu. "The Application of the J-Integral to Problems of Crack Bridging". Acta Metall. Mater. 42 [6] 1805-1810 (1994).
61. G.A. Gogotsi, Y.L. Groushevsky, K.K. Strelov. "The Significance of Non-Elastic Deformation in the Fracture of Heterogeneous Ceramic Materials". Ceramurg. Int. 4 [3] 113-118 (1978).
62. M. Elices, G.V. Guinea, J. Gomez, J. Planas. "The cohesive zone model: advantages, limitations and challenges". Eng. Fract. Mech. 69 [2] 137-163 (2002).
63. R.W. Davidge, G. Tappin. "The Effective Surface Energy of Brittle Materials". J. Mater. Sci. 3 165-173 (1968).
64. J. Nakayama. "Direct Measurement of Fracture Energies of Brittle Heterogeneous Materials". J. Am. Ceram. Soc. 48 [11] 538-87 (1965).
65. H.G. Tattersall, G. Tappin. "The Work of Fracture and its Measurement in Metals, Ceramics and other Materials". J. Mater. Sci. 1 296-301 (1966).
66. W. Kreher, W. Pompe. "Increased Fracture Toughness of Ceramics by Energy-Dissipative Mechanisms". J. Mater. Sci. 16 694-706 (1981).
67. A.S. Jayatilaka. "Fracture Toughness", p. 257-274 in Fracture of Engineering Brittle Materials. Applied Science Publishers Ltd., London (UK) 1979.
68. J. Y. Pastor, J. Planas, M. Elices. "Ambient and High-Temperature Stable Fracture Tests in Ceramics: Applications to Ytria-Partially-Stabilized Zirconia". J. Am. Ceram. Soc. 76 [11] 2927-29 (1993).
69. D.B. Binns, P. Popper. "Mechanical Properties of Some Commercial Alumina Ceramics", p. 71-82 in Proceedings of the British Ceramic Society, 6: Mechanical Properties of Non-metallic Crystals and Polycrystals. Ed. British Ceramic Society, London-Stoke-on-Trent (UK) 1966.
70. O. Sbaizero, G. Pezzotti, T. Nishida. "Fracture Energy and R-Curve Behavior of Al_2O_3/Mo Composites". Acta Mater. 46 [2] 681-687 (1998).
71. S.M. Wiederhorn. "Fracture of Sapphire". J. Am. Ceram. Soc. 52 [9] 485 (1969).
72. G.R. Anstis, P. Chantikul, B.R. Lawn, D.B. Marshall. "A Critical Evaluation of Indentation Techniques for Measuring Fracture Toughness: I, Direct Crack Measurements". J. Am. Ceram. Soc. 64 [9] 533-538 (1981).
73. P. Chantikul, G.R. Anstis, B.R. Lawn, D.B. Marshall. "A Critical Evaluation of Indentation Techniques for Measuring Fracture Toughness: II, Strength Method". J. Am. Ceram. Soc. 64 [9], 539-543 (1981).
74. G.M. Pharr, W.C. Oliver, F.R. Brotzen. "On the generality of the relationship among contact stiffness, contact area and elastic modulus during indentation". J. Mater. Res. 7 [3] 613-617 (1992).
75. S. Bueno, C. Baudín. "Instrumented Vickers microindentation of alumina based materials". J. Mater. Res. 21 [1] 161-173 (2006).
76. I. Bar-On, F.I. Baratta, K. Cho. "Crack Stability and Its Effect on Fracture Toughness of Hot-Pressed Silicon Nitride Beam Specimens". J. Am. Ceram. Soc. 79 [9] 2300-308 (1996).
77. A.S. Jayatilaka. "Stress Intensity Factor", p. 19-29 in Fracture of Engineering Brittle Materials. Applied Science Publishers Ltd., London (UK) 1979.
78. J.Y. Pastor, J.Y. Planas, M. Elices. "Ensayos de fractura estables en materiales cerámicos". Bol. Soc. Esp. Ceram. V., 31 [4] 322-325 (1992).
79. R. Damani, R. Gstrein, R. Danzer. "Critical Notch-Root Radius Effect in SENB-S Fracture Toughness Testing". J. Eur. Ceram. Soc. 16 695-702 (1996).
80. H. Awaji, Y. Sokaida. "V-Notch Technique for Single-Edge Notched Beam and Chevron Notch Methods". J. Am. Ceram. Soc. 73 [11] 3522-23 (1990).
81. T. Nishida, Y. Hanaki, G. Pezzotti. "Effect of Notch-Root Radius on the Fracture Toughness of a Fine-Grained Alumina". J. Am. Ceram. Soc. 77 [12] 606-608 (1994).
82. J. Kübler. "Fracture toughness of ceramics using the SEVNB method: preliminary results". Ceram. Eng. Sci. Proc. 18 [4] 155-62 (1997).
83. F.I. Baratta, W.A. Dunlay. "Crack Stability in Simply Supported Four-Point and Three-Point Loaded Beams of Brittle Materials". Mech. Mater. 10 149-159 (1990).
84. B. Mussler, M.V. Swain, N. Claussen. "Dependence of Fracture Toughness of Alumina on Grain Size and Test Technique". J. Am. Ceram. Soc. 65 [11] 566-572 (1982).
85. S. Bueno, C. Baudín. "Layered materials with high strength and flaw tolerance based on alumina and aluminium titanate". J. Eur. Ceram. Soc. 27 [2-3] 1455-1462 (2007).
86. G.V. Guinea, J.Y. Pastor, J. Planas, M. Elices. "Stress intensity factor, compilance and CMOD for a general three-point-bend beam". Int. J. Fract. 89 103-116 (1998).
87. C. Droillard, J. Lamon. "Fracture Toughness of 2-D Woven SiC/SiC CVI-Composites with Multilayered Interphases". J. Am. Ceram. Soc. 79 [4] 849-858 (1996).
88. T. Hashida, C. Li, H. Takahashi. "New Development of the J-Based Fracture Testing Technique for Ceramic-Matrix Composites". J. Am. Ceram. Soc. 77 [6] 1553-1561 (1994).
89. H. Hübner, W. Jillek. "Sub-critical crack extension and crack resistance in polycrystalline alumina". J. Mater. Sci. 12 117-125 (1977).
90. K. Tanaka, Y. Akiniwa, H. Kimachi, Y. Kita. "R-curve behaviour in fracture of notched porous ceramics". Eng. Fract. Mech. 70 [9] 1101-1113 (2003).
91. M. E. Ebrahimi, J. Chevalier, G. Fantozzi. "R-curve evaluation and bridging stress determination in alumina by compliance analysis". J. Eur. Ceram. Soc. 23 [6] 943-949 (2003).
92. H. Wieninger, K. Kromp, R.F. Pabst. "Crack resistance curves of alumina and zirconia at room temperature". J. Mater. Sci. 21 411-418 (1986).)

Recibido: 08.06.06
Aceptado: 13.12.06

◆ ◆ ◆